Chinese Journal of Natural Medicines

Diterpenoids and lignans from fossil Chinese medicinal succinum and their activity against renal fibrosis

Yefei Chen, Yunfei Wang, Yunyun Liu, Yongming Yan, Yongxian Cheng

Citation: Yefei Chen, Yunfei Wang, Yunyun Liu, Yongming Yan, Yongxian Cheng, Diterpenoids and lignans from fossil Chinese medicinal succinum and their activity against renal fibrosis, Chinese Journal of Natural Medicines, 2025, 23(7), 888−896. doi: 10.1016/S1875−5364(25)60916−2.

View online: https://doi.org/10.1016/S1875−5364(25)60916−2

Chinese Journal of Natural Medicines 23 (2025) 888-896

Contents lists available at ScienceDirect

Chinese Journal of Natural Medicines

journal homepage: www.cjnmcpu.com/

Original article

Diterpenoids and lignans from fossil Chinese medicinal succinum and their activity against renal fibrosis

Yefei Chen[a,b], Yunfei Wang[a], Yunyun Liu[a], Yongming Yan[a], Yongxian Cheng[a,b,*]

[a] *Guangdong Provincial Key Laboratory of Chinese Medicine Ingredients and Gut-Microbiomics, Institute for Inheritance-Based Innovation of Chinese Medicine, Marshall Laboratory of Biomedical Engineering, School of Pharmacy, Shenzhen University Medical School, Shenzhen University, Shenzhen 518055, China*

[b] *Guangdong Key Laboratory for Biomedical Measurements and Ultrasound Imaging, National-Regional Key Technology Engineering Laboratory for Medical Ultrasound, School of Biomedical Engineering, Shenzhen University Medical School, Shenzhen 518060, China*

ARTICLE INFO

Article history:
Received 12 August 2024
Revised 23 November 2024
Accepted 27 January 2025
Available online 20 July 2025

Keywords:
Succinum
Lignan
Diterpenoid
Renal fibrosis

ABSTRACT

Five previously undescribed diterpenoids, named succipenoids D–H (**1**–**5**), along with four undescribed lignans, named succignans A–D (**6**–**9**), were isolated from the dichloromethane extract of Chinese medicinal succinum. Compounds **1**–**5** were characterized as nor-abietane diterpenoids, while compounds **6**–**9** were identified as lignans polymerized from two groups of phenylpropanoid units. The structures of these novel compounds, including their absolute configurations, were determined through spectroscopic and computational methods. Biological assessments of renal fibrosis demonstrated that compounds **6** and **7** effectively reduce the expression of proteins associated with renal fibrosis, including α-smooth muscle actin (α-SMA), collagen I, and fibronectin in transforming growth factor-β1 (TGF-β1) induced normal rat kidney proximal tubular epithelial cells (NRK-52e).

1. Introduction

Chinese medicinal materials derived from fossils are unique because they originate from plants and animals buried underground for centuries. Succinum is an organic substance formed through complex geological processes from the resins of coniferous and leguminous plants that flourished during the Mesozoic Cretaceous to Cenozoic Tertiary periods [1]. Succinum is primarily harvested from various regions in Russia, Myanmar, and China, particularly in the provinces of Henan, Liaoning, and Yunnan [2]. The chemical composition of succinum encompasses multiple components, with resin and volatile oils as the primary constituents. The resin consists mainly of alcohol-soluble compounds, including succinoabietic acid, succinoabietinolic acid, and succinoabietol, as well as alcohol-insoluble components such as succinin, succinoresinol, and succinoresinol succinate [3]. Furthermore, the volatile compounds in succinum primarily comprise monoterpenes, sesquiterpenes, diterpenes, and aromatic compounds [4]. Succinum exhibits diverse morphological characteristics, appearing in transparent and translucent varieties with colors ranging from yellow and orange to brown, and occasionally red. The specimen examined in this study is illustrated in Fig. 1. Beyond its aesthetic value, succinum represents a significant fossil Chinese medicinal material extensively utilized in clinical applications [5]. Traditional Chinese medicine has utilized succinum for thousands of years to promote mental relaxation, enhance blood circulation, and alleviate blood stagnation [6]. Recent research has demonstrated succinum's anti-bacterial [7], anti-inflammatory [8], and anti-allergenic properties [9]. As a continuation of our research on bioactive compounds from medicinal plant resins [10-12], nine new compounds (**1**–**9**) (Fig. 2) were isolated and characterized from succinum. The structures of these newly identified compounds were determined through comprehensive spectroscopic analysis. Additionally, their efficacy against renal fibrosis was evaluated.

2. Results and discussion

2.1. Structure elucidation of the compounds

Compound **1** was isolated as a colorless oil. Its molecular formula was established as $C_{22}H_{32}O$ with 7 degrees of unsaturation based on high-resolution electrospray ionization mass spectrometry (HR-ESI-MS) (*m/z* 313.2523 $[M + H]^+$, Calcd. for $C_{22}H_{33}O$, 313.2526), ^{13}C nuclear magnetic resonance (NMR), and distortionless enhancement by polarization transfer (DEPT) spectra. The ^1H NMR spectrum (Table 1) revealed a mono-substituted benzene ring [δ_H 7.29 (2H, m, H-19, H-21), 7.22 (2H, m, H-18, H-22), and 7.19 (1H, m, H-20)], and three aliphatic methyls [δ_H 1.65 (3H, s, H-14), 1.01 (3H, s, H-12), and 0.94 (3H, s, H-13)]. Analysis of the ^{13}C NMR and heteronuclear single quantum correlation (HSQC) spectra indicated three methyls, eight methylenes (one oxygenated), six methines (one sp^3 and five sp^2), and five non-protonated carbons. Comparison with literature data suggested that compound **1** shares structural similarities with luffarin-O [13], differing in the replacement of a methyl with a hydroxymethyl-

* Corresponding author.
E-mail address: yxcheng@szu.edu.cn

https://doi.org/10.1016/S1875-5364(25)60916-2

Fig. 1 The morphology of succinum.

ene at C-4, and the transformation of the C-16 substituent into a benzene ring. This structural assignment was confirmed by heteronuclear multiple bond correlation (HMBC) (Fig. 3) of H_3-12/C-3, C-4, C-5, C-11, H_2-11/C-3, and H_2-16/C-15, C-17, C-18, C-22. The molecule contains three chiral centers. Rotating-frame Overhauser effect spectroscopy (ROESY) correlations of H_3-13/H_2-11, Ha-7 and H-5/Hb-7, combined with molecular model analysis, established the relative configurations at C-4, C-5, and C-10 as $4S^*$,$5R^*$,$10S^*$ (Fig. 4). The absolute configuration was determined through comparison of calculated and experimental electronic circular dichroism (ECD) spectra. The calculated ECD spectrum of (4*S*,5*R*,10*S*)-**1** demonstrated good agreement with the experimental spectrum (Fig. 5), confirming the absolute configuration of **1** as 4*S*,5*R*,10*S*. Therefore, compound **1** was characterized and designated as succipenoid D.

Compound **2** was isolated as a colorless oil. Its molecular formula, $C_{16}H_{24}O_2$, indicating five degrees of unsaturation, was established based on HR-ESI-MS (*m/z* 249.1843 $[M + H]^+$, Calcd. for $C_{16}H_{25}O_2$, 249.1849), ^{13}C NMR, and DEPT spectra. The ^1H NMR spectrum (Table 2) exhibited an olefin proton [δ_H 5.84 (1H, br s, H-13)], an oxygenated methylene [δ_H 3.76 (1H, d, *J* = 10.8 Hz, Ha-14), and 3.46 (1H, br d, *J* = 10.8 Hz, Hb-14)], and two methyls [δ_H 1.05 (3H, s, H-15), and 0.65 (3H, s, H-16)]. The ^{13}C NMR and HSQC spectra revealed 16 carbons, comprising two methyls, seven methylenes (one oxygenated), three methines (two sp^3 and one sp^2), and four non-protonated carbons. The NMR spectra match those of (−)-1,4,5,5a,6,7,8,9,9a,9b-decahydro-6,6,9a-trimethyl-[5a*S*-(5a*α*,9a*β*,9b*α*)]-2*H*-benz(e)inden-2-one [14], except for the absence of a methyl and the presence of an additional oxygenated methine at C-4 in **2**. This structure was confirmed by the HMBC (Fig. 3) H_2-14/C-3, C-4, C-5, C-15. Therefore, the planar structure of compound **2** was established as shown in Fig. 2. The relative configuration of **2** was determined through ROESY correlations (Fig. 4). The correlations of H-9/H-5, Hb-1 indicated that H-5 and H-9 are positioned on the same side. Furthermore, the ROESY correlations of H_3-16/H_2-14, Ha-1 demonstrate that H_2-14 and H_3-16 are on the opposite face. Consequently, the relative configuration of **2** was assigned as $4S^*$,$5R^*$,$9S^*$,$10R^*$. To determine the absolute configuration of **2**, ECD calculations were performed. The comparison of experimental and calculated ECD spectra (Fig. 5) confirmed the absolute configuration of **2** as 4*S*,5*R*,9*S*,10*R*, and compound **2** was subsequently named succipenoid E.

Compound **3** was isolated as a colorless oil. Its molecular formula, $C_{16}H_{24}O_2$, indicating five degrees of unsaturation, was established as based on HR-ESI-MS (*m/z* 249.1844 $[M + H]^+$, Calcd. for $C_{16}H_{25}O_2$, 249.1849), ^{13}C NMR, and DEPT spectra. The ^1H NMR spectrum (Table 2) revealed an olefinic proton [δ_H 5.70 (1H, br s, H-11)], two oxygenated methylene [δ_H 3.80 (1H, d, *J* = 10.9 Hz, Ha-14), and 3.55 (1H, d, *J* = 10.9 Hz, Hb-14)], and two methyls [δ_H 1.16 (3H, s, H-16), and 0.99 (3H, s, H-15)]. The ^{13}C NMR and HSQC spectra exhibited 16 carbons, comprising two methyls, seven methylenes (one oxygenated), three methines (two sp^3 and one sp^2), and four non-protonated carbons. The NMR spectra of **3** demonstrated similarity to the known compound, (−)-3,3a,4,5,5a,6,7,8,8,9,9a-decahydro-6,6,9a-trimethyl-(3a*S*-(3a*β*,5a*α*,9a*β*)-2*H*-benz(e)inden-2-one [14]. The absence of a methyl and presence of an additional oxygenated methine at C-4 in **3** was confirmed through HMBCs (Fig. 3) of H_2-14/C-4, C-5, C-15 and H_3-15/C-4, C-5, C-14. The ROESY correlations (Fig. 4) of H_3-15/H-5, H_3-16/H_2-14, H-8 indicated that H_3-15 and H-5 share the same orientation, while H_3-16, H_2-14 and H-8 are positioned on the opposite face. Consequently, the relative configuration of **3** was established as $4S^*$,$5R^*$,$8S^*$,$10S^*$. Following the same procedure as **2**, the absolute configuration of **3** was determined as 4*S*,5*R*,8*S*,10*S* based on ECD calculations (Fig. 5). Thus, compound **3** was conclusively characterized and named succipenoid F.

Compound **4** was isolated as a colorless oil. Its molecular formula, $C_{16}H_{24}O_3$, was established through HR-ESI-MS (*m/z*

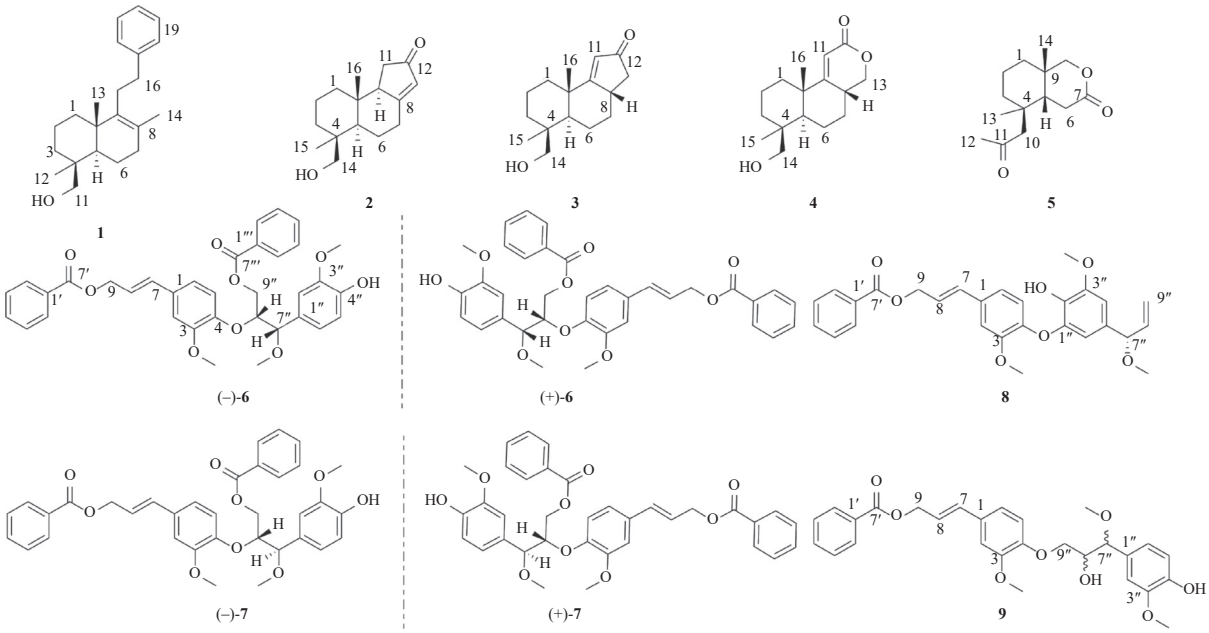

Fig. 2 Structures of compounds **1**–**9**.

Table 1 ^{1}H (600 MHz) and ^{13}C NMR (150 MHz) data for **1** (*J* in Hz, in $CDCl_3$).

No.	δ_C	δ_H	No.	δ_C	δ_H
1	37.2, CH_2	Ha: 1.99, m Hb: 1.32, m	11	65.6, CH_2	Ha: 3.78, d (10.9) Hb: 3.47, d (10.9)
2	19.4, CH_2	Ha: 1.78, m Hb: 1.59, m	12	26.9, CH_3	1.01, s
3	35.4, CH_2	Ha: 1.83, m Hb: 0.98, m	13	20.7, CH_3	0.94, s
4	38.8, C		14	19.7, CH_3	1.65, s
5	52.7, CH	1.35, m	15	30.8, CH_2	Ha: 2.30, m Hb: 2.16, m
6	18.9, CH_2	1.44, m	16	36.9, CH_2	2.64, m
7	34.1, CH_2	Ha: 2.07, td (11.0, 5.6) Hb: 1.95, m	17	143.3, C	
8	126.5, C		18, 22	128.2, CH	7.22, m
9	140.0, C		19, 21	128.5, CH	7.29, m
10	39.1, C		20	125.8, CH	7.19, m

265.1789 $[M + H]^+$, Calcd. for $C_{16}H_{25}O_3$, 265.1798), ^{13}C NMR, and DEPT spectra. The ^{1}H NMR spectrum (Table 3) revealed an olefin proton [δ_H 5.76 (1H, s, H-11)], two oxygenated methylenes [δ_H 4.38 (1H, dd, *J* = 11.2, 5.7 Hz, Ha-13), and 3.89 (1H, t, *J* = 11.2 Hz, Hb-13); δ_H 3.78 (1H, d, *J* = 10.9 Hz, Ha-14), and 3.52 (1H, d, *J* = 10.9 Hz, Hb-14)], and two methyls [δ_H 1.12 (3H, s, H-16), and 1.00 (3H, s, H-15)]. The ^{13}C NMR and HSQC spectra exhibited 16 carbons, comprising two methyls, seven methylenes (two oxygenated), three methines (2 sp^3 and 1 sp^2), and four non-protonated carbons. The NMR spectra of **4** demonstrated close similarity to those of compound **3**, with the primary difference being the insertion of an oxygen between C-12 and C-13 in **4** to form a conjugated lactone. This structure was confirmed by the HMBC (Fig. 3) of H_2-13/C-9, C-12, H-8/C-11, and H-11/C-12 and the deshielded carbonyl chemical shift (δ_C 166.3), establishing the planar structure of compound **4**. The ROESY correlations (Fig. 4) of H_3-15/H-5, H-8/H_3-16, and H_3-16/H_2-14 indicated that H-5 and H_3-15 share the same orientation, while H-8, H_2-14, and H_3-16 are oriented in the opposite face. ECD calculations were conducted to determine the absolute configuration. The analysis revealed the absolute configuration as 4*S*,5*R*,8*R*,10*S* based on the comparison of experimental and calculated ECD curves (Fig. 5), and compound **4** was consequently named succipenoid G.

Compound **5** was isolated as a colorless oil. Its molecular formula, $C_{14}H_{22}O_3$, indicating four degrees of unsaturation, was established based on HR-ESI-MS (*m*/*z* 239.1642 $[M + H]^+$, Calcd. for $C_{14}H_{23}O_3$, 239.1642), ^{13}C NMR, and HSQC spectra. The ^{1}H NMR spectrum (Table 3) of **5** revealed resonances for three aliphatic methyl groups at δ_H 2.13 (s), 1.13 (s), and 1.03 (s) and two oxygenated methylene protons [δ_H 4.38 (1H, d, *J* = 11.8 Hz, Ha-8), and 3.90 (1H, d, *J* = 11.8 Hz, Hb-8)]. The ^{13}C NMR and DEPT spectra indicated 14 carbons comprising three methyls, six methylenes (one oxygenated), one methine, and four non-protonated carbons (including two carbonyls). The ^{1}H–^{1}H correlation spectroscopy (COSY) correlations (Fig. 3) of H-1/H-2/H-3 and H-5/H-6 demonstrated two structure fragments. The HMBCs (Fig. 3) of H-3/C-1, C-2, C-4, C-5, H-5/C-7, H_3-12/C-10, C-11, H_3-13/C-4, C-5, C-10, and H_3-14/C-1, C-5, C-8, C-9 established that compound **5** contains two six-membered rings including a lactone, two methyls at C-4 and C-9 and a propanone attached to C-4 *via* C-C bond formation. The relative configuration of **5** was determined through ROESY correlations (Fig. 4) of H_3-13/Hb-6 and H_3-14/H-5, Ha-6, indicating that H-5 and H_3-14 are co-facial, while H_3-13 is oriented on the opposite face. Following the approach used for the previously described compounds, ECD calculations (Fig. 5) for (4*R*,5*R*,9*S*)-**5** showed curve accordance with experimental data, confirming the absolute configuration of **5** as 4*R*,5*R*,9*S*. Consequently, compound **5** was designated as succipenoid H.

Compounds **6** and **7** were obtained as yellowish oils, isolated as a pair of diastereomers and subsequently separated into two pairs of enantiomers (+)-**6**/(−)-**6** and (+)-**7**/(−)-**7**. Both compounds **6** and **7** were confirmed to possess identical molecular

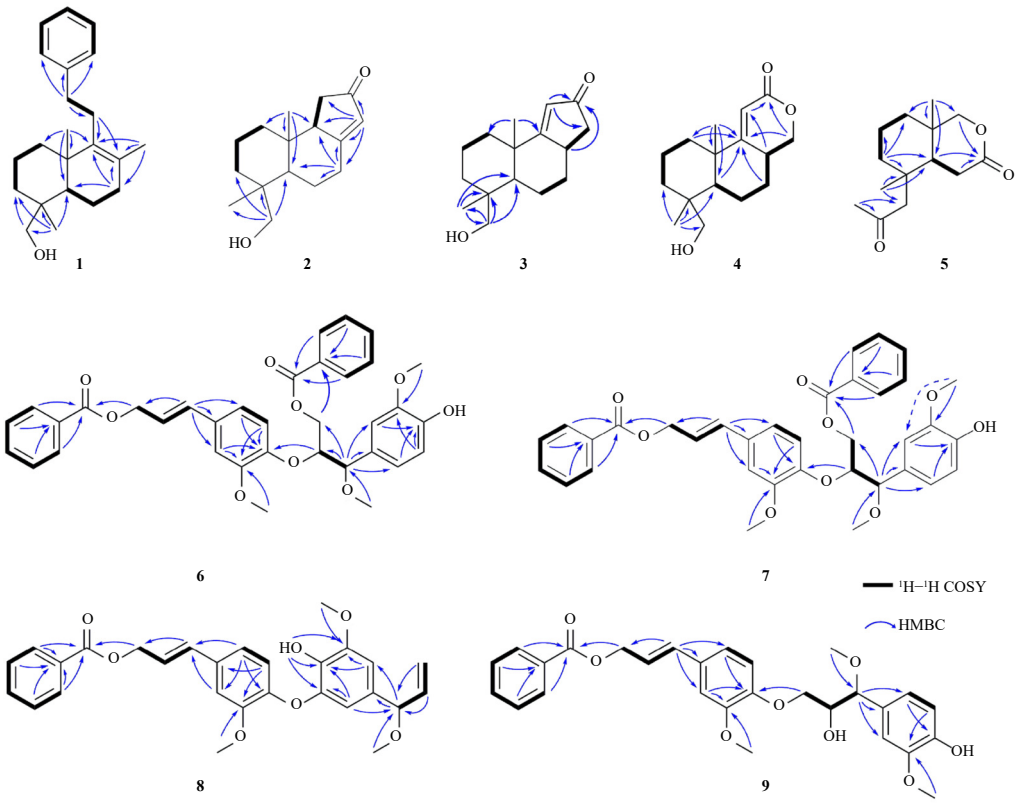

Fig. 3 Key ^{1}H–^{1}H COSY and HMBC correlations of **1**–**9**.

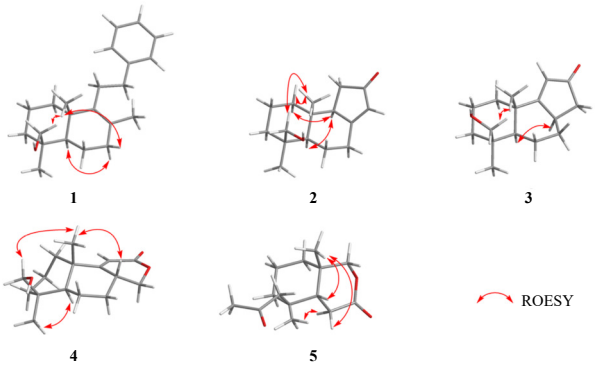

Fig. 4 Key ROESY correlations of **1**–**5**.

formulas of $C_{35}H_{34}O_9$ through analysis of compound **6** by HR-ESI-MS, *m/z* 621.2076 $[M + Na]^+$ (Calcd. as 621.2095) and compound **7** by HR-ESI-MS, *m/z* 621.2074 $[M + Na]^+$ (Calcd. as 621.2095).

The ^{1}H NMR spectrum (Table 4) of **6** revealed two mono-substituted benzene rings [δ_H 8.08 (2H, br d, *J* = 8.3 Hz, H-2‴, H-6‴), 7.45 (2H, br t, *J* = 8.3 Hz, H-3‴, H-5‴), 7.56 (1H, br t, *J* = 8.3 Hz, H-4‴); 7.84 (2H, br d, *J* = 8.3 Hz, H-2′, H-6′), 7.36 (2H, br t, *J* = 8.3 Hz, H-3′, H-5′), and 7.49 (1H, br t, *J* = 8.3 Hz, H-4′)], two tri-substituted benzene rings [δ_H 6.97 (1H, d, *J* = 1.6 Hz, H-2″), 6.89 (1H, d, *J* = 8.1 Hz, H-5″); 6.92 (1H, dd, *J* = 8.1, 1.6 Hz, H-6″); 6.85 (1H, d, *J* = 2.0 Hz, H-2), 6.75 (1H, d, *J* = 8.1 Hz, H-5), and 6.84 (1H, dd, *J* = 8.1, 2.0 Hz, H-6)], a set of *trans* double bond signals [δ_H 6.63 (1H, br d, *J* = 15.8 Hz, H-7), and 6.25 (1H, dt, *J* = 15.8, 6.5 Hz, H-8)], and three methoxy signals [δ_H 3.70 (3H, s, 3-OCH_3), 3.85 (3H, s, 3″-OCH_3), and 3.31 (3H, s, 7″-OCH_3)]. The ^{13}C NMR data indicated 35 carbons, comprising three methoxy methyls, two sp^3 methylene, twenty methines (including eighteen sp^2 and two oxygenated sp^3), and ten non-protonated carbons (two carbonyls and eight sp^2 including four oxygenated). The NMR spectra of **6** and **7** exhibit similarities to tonkinensisin A [15], with the distinction that compounds **6** and **7** contain a *trans* double bond, as evidenced by long-range coupling constants, $J_{7,8}$ = 15.8 and 15.7 Hz, respectively. Furthermore, the planar structures of **6** and **7** were established through comprehensive two-dimensional (2D) NMR data analysis, specifically the ^{1}H–^{1}H COSY and HMBC (Fig. 3).

Compound **6**, exhibiting a smaller $^3J_{HH}$ value (4.9 Hz), was characterized as having an *erythro* configuration, while compound **7**, displaying a larger $^3J_{HH}$ value (6.0 Hz), was identified as having a *threo* configuration (Table 4) [16-18]. The absolute configurations of **6** and **7** were established as (7″*S*,8″*R*)-(−)-**6**, (7″*R*,8″*S*)-(+)-**6**, (7″*R*,8″*R*)-(−)-**7** and (7″*S*,8″*S*)-(+)-**7** through ECD calculations (Fig. 5). Consequently, the structures of (±)-**6** and (±)-**7** were designated as (±) succignan A and (±) succignan B, respectively.

Compound **8** was isolated as a yellowish oil. Its molecular formula was established as $C_{28}H_{28}O_7$ based on HR-ESI-MS (*m/z* 499.1733 $[M + Na]^+$, Calcd. for $C_{28}H_{28}O_7Na$, 499.1727), ^{13}C NMR, and HSQC spectra. The ^{1}H NMR spectrum (Table 5) revealed a mono-substituted benzene ring [δ_H 8.08 (2H, br d, *J* = 7.7 Hz, H-2′, H-6′), 7.45 (2H, br t, *J* = 7.7 Hz, H-3′, H-5′), and 7.57 (1H, br t, *J* = 7.4 Hz, H-4′)], a tri-substituted benzene ring [δ_H 7.04 (1H, d, *J* = 1.9 Hz, H-2), 6.92 (1H, dd, *J* = 8.3, 1.9 Hz, H-6), and 6.86 (1H, d, *J* = 8.3 Hz, H-5)], a tetra-substituted benzene ring [δ_H 6.68 (1H, d, *J* = 1.9 Hz, H-4″), and 6.54 (1H, d, *J* = 1.9 Hz, H-6″)], a terminal double bond [δ_H 5.85 (1H, ddd, *J* = 17.0, 10.3, 6.6 Hz, H-8″), and 5.19 (1H, m, H-9″)], a *trans* olefin [δ_H 6.70 (1H, d, *J* = 15.9 Hz, H-7), and 6.33 (1H, dt, *J* = 15.9, 6.4 Hz, H-8)], and three methoxy methyls [δ_H 3.89 (3H, s, 3-OCH_3), 3.92 (3H, s, 3″-OCH_3), and 3.27 (3H, s, 7″-OCH_3)]. The ^{13}C NMR and HSQC spectra indicated 28 carbon signals, comprising three methoxy groups, two sp^3 methylene, fourteen methines (including thirteen sp^2 and one oxygenated sp^3), and nine non-protonated carbons (one carbonyl and eight sp^2 including five oxygenated). The structure of **8** was elucidated primarily through 2D NMR spectroscopic data. The ^{1}H–^{1}H COSY correlations (Fig. 3) of H-9/H-8/H-7, and H-9″/H-8″/H-7″ and the HMBC correlations (Fig. 3) of H-7/C-9, H-2, H-6/C-7, H-6″, H-8″, H-9″/C-7″, H-2′, H-6′, H-9/C-7′, and H-2″-OH/C-1″, C-3″ indicated the presence of two phenylpropanoid units connected *via* an oxygen bridge between C-4 and C-1″ of these phenylpropanoid rings, with a benzoate group attached at the C-9 position of one phenylpropanoid unit. The HMBC of 3-OCH_3/C-3, 3″-OCH_3/C-3″, and 7″-OCH_3/C-7″ confirmed the presence of three methoxy substituents at C-3, C-3″, and C-7″. Thus, the planar structure of compound **8** was determined. Compound **8** has two same moieties [I (C_1–C_9) and II ($C_{1''}$–$C_{9''}$)] as that of 1-[(7*R*)-hydroxy-8-propenyl1-3-[3′-methoxy-1′-(8′-propenyl)-phenoxy]-4-hydroxy-5-methoxybenzene [19] and their similar CD spectra established the absolute configuration at C-7″ of **8** as *R*. This determination was further corroborated by the calculated ECD spectrum of (7″*R*)-**8** matching the experimental spectrum (Fig. 5).

Compound **9** was obtained as a colorless gum. Its molecular formula, $C_{28}H_{30}O_8$, indicating 14 degrees of unsaturation, was established based on HR-ESI-MS (*m/z* 517.1819 $[M + Na]^+$, Calcd. for $C_{28}H_{30}O_8Na$, 517.1833), ^{13}C NMR, and DEPT spectra. The ^{1}H NMR spectrum (Table 5) indicated a mono-substituted benzene ring [δ_H 8.08 (2H, br d, *J* = 8.5 Hz, H-2′, H-6′), 7.45 (2H, br t, *J* = 8.5 Hz, H-3′, H-5′), and 7.56 (1H, br t, *J* = 8.5 Hz, H-4′)], two tri-substituted benzene rings [δ_H 6.95 (1H, d, *J* = 2.0 Hz, H-2), 6.87 (1H, dd, *J* = 8.2, 2.0 Hz, H-6), 6.70 (1H, d, *J* = 8.2 Hz, H-5), 6.83 (2H, d, *J* = 2.0 Hz, H-2″), 6.87 (1H, d, *J* = 8.0 Hz, H-5″), and 6.84 (1H, dd, *J* = 8.0, 2.0 Hz, H-6″)], a *trans*-alkene [δ_H 6.65 (1H, br d, *J* = 15.8 Hz, H-7), and 6.28 (1H, dt, *J* = 15.8, 6.6 Hz, H-8), and three methoxy methyls [δ_H 3.87 (3H, s, 3-OCH_3), 3.79 (3H, s, 3″-

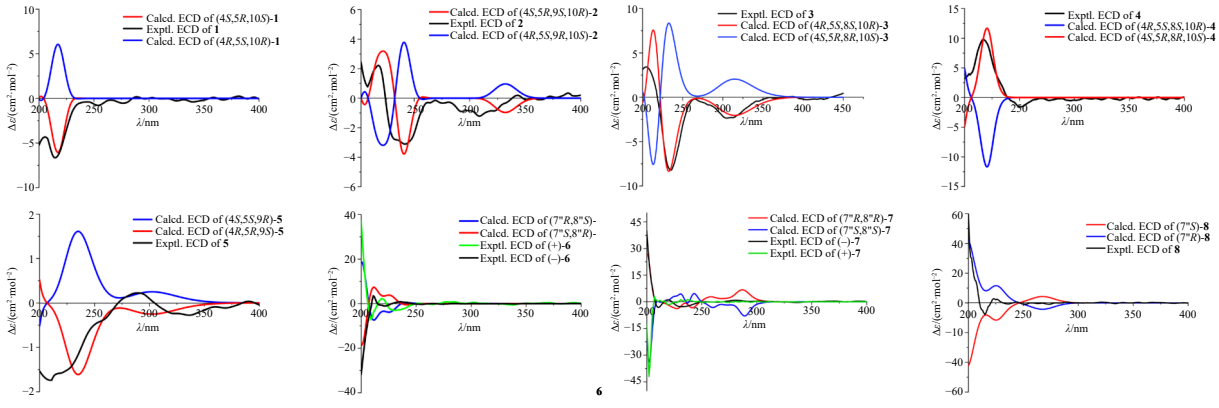

Fig. 5 Experimental and calculated ECD spectra of compounds **1**–**8**.

Table 2 ^{1}H (600 MHz) and ^{13}C NMR (150 MHz) data for **2** and **3** (*J* in Hz, in $CDCl_3$).

No.	2		3	
	δ_C	δ_H	δ_C	δ_H
1	40.3, CH_2	Ha: 1.62, m Hb: 1.21, m	37.1, CH_2	Ha: 1.77, m Hb: 1.57, m
2	18.4, CH_2	1.50, overlap	18.2, CH_2	Ha: 1.65, m Hb: 1.58, overlap
3	35.7, CH_2	Ha: 1.89, m Hb: 1.04, m	35.5, CH_2	Ha: 1.87, m Hb: 1.00, m
4	39.1, C		39.3, C	
5	54.3, CH	1.43, dd (12.9, 2.2)	54.2, CH	1.19, m
6	22.6, CH_2	Ha: 2.00, ddt (12.5, 6.3, 2.2) Hb: 1.50, overlap	21.5, CH_2	Ha: 1.82, m Hb: 1.58, overlap
7	31.2, CH_2	Ha: 2.85, ddd (14.5, 4.5, 2.2) Hb: 2.27, m	36.2, CH_2	Ha: 2.24, ddt (12.5, 6.2, 3.2) Hb: 1.05, m
8	182.5, C		38.5, CH	2.89, m
9	55.7, CH	2.49, dd (6.5, 2.3)	194.4, C	
10	38.6, C		39.3, C	
11	36.4, CH_2	Ha: 2.23, dd (18.8, 6.5) Hb: 2.14, dd (18.8, 2.3)	122.3, CH	5.70, br s
12	209.8, C		209.7, C	
13	127.8, CH	5.84, br s	42.5, CH_2	Ha: 2.54, dd (18.8, 6.5) Hb: 1.95, dd (18.8, 2.2)
14	65.1, CH_2	Ha: 3.76, d (10.8) Hb: 3.46, br d (10.8)	65.3, CH_2	Ha: 3.80, d (10.9) Hb: 3.55, d (10.9)
15	27.2, CH_3	1.05, s	27.0, CH_3	0.99, s
16	13.7, CH_3	0.65, s	20.2, CH_3	1.16, s

Table 3 ^{1}H (600 MHz) and ^{13}C NMR (150 MHz) data for **4** and **5** (*J* in Hz, in $CDCl_3$).

No.	4		5	
	δ_C	δ_H	δ_C	δ_H
1	35.3, CH_2	Ha: 1.85, m Hb: 1.46, m	33.6, CH_2	Ha: 1.49, m Hb: 1.29, m
2	18.2, CH_2	1.62, m	17.8, CH_2	1.54, m
3	36.1, CH_2	Ha: 1.89, m Hb: 1.80, m	35.7, CH_2	Ha: 1.67, m Hb: 1.54, m
4	39.2, C		31.6, C	
5	53.1, CH	1.20, dd (12.8, 2.6)	43.2, CH	1.93, dd (8.0, 3.3)
6	20.5, CH_2	Ha: 1.85, m Hb: 1.62, m	28.6, CH_2	Ha: 2.68, dd (18.6, 8.0) Hb: 2.49, dd (18.6, 3.3)
7	30.2, CH_2	Ha: 2.00, m Hb: 1.07, m	171.2, C	
8	32.4, CH_2	2.73, m	76.7, CH_2	Ha: 4.38, d (11.8) Hb: 3.90 d (11.8)
9	172.7, C		37.1, C	
10	40.3, C		54.3,CH_2	Ha: 2.54, d (15.6) Hb: 2.33, d (15.6)
11	110.2, CH	5.76, s	208.2, C	
12	166.3, C		33.1, CH_3	2.13, s
13	70.8, CH_2	Ha: 4.38, dd (11.2, 5.7) Hb: 3.89, t (11.2)	21.5, CH_3	1.03, s
14	65.4, CH_2	Ha: 3.78, d (10.9) Hb: 3.52, d (10.9)	28.8, CH_3	1.13, s
15	27.0, CH_3	1.00, s		
16	21.9, CH_3	1.12, s		

OCH_3), and 3.28 (3H, s, 7″-OCH_3)]. The ^{13}C NMR and HSQC spectra revealed 28 carbons corresponding to three oxymethyls, two methylenes (two oxygenated), fifteen methines (13 olefinic and two oxygenated), and eight non-protonated carbons (including

Table 4 ^{1}H (600 MHz) and ^{13}C NMR (150 MHz) data for **6** and **7** (*J* in Hz, in $CDCl_3$).

No.	6		7	
	δ_C	δ_H	δ_C	δ_H
1	131.3, C		131.1, C	
2	110.1, CH	6.85, d (2.0)	110.0, CH	6.90, d (2.0)
3	151.0, C		150.9, C	
4	148.2, C		148.7, C	
5	118.7, CH	6.75, d (8.1)	118.3, CH	6.98, d (8.1)
6	119.9, CH	6.84, dd (8.1, 2.0)	120.0, CH	6.89, overlap
7	134.3, CH	6.63, br d (15.8)	134.4, CH	6.66, dd (15.7, 1.3)
8	122.0, CH	6.25, dt (15.8, 6.5)	121.9, CH	6.27, dt (15.7, 6.5)
9	65.7, CH_2	4.96, br d (6.5)	65.8, CH_2	4.96, dd (6.5, 1.3)
1′	130.0, C		129.6, C	
2′, 6′	129.7, CH	7.84, br d (8.3)	129.7, CH	7.85, br d (7.7)
3′, 5′	128.3, CH	7.36, br t (8.3)	128.4, CH	7.37, br t (7.7)
4′	133.0, CH	7.49, br t (8.3)	133.1, CH	7.50, br t (7.7)
7′	166.5, C		166.3, C	
1″	130.0, C		130.3, C	
2″	109.9, CH	6.97, d (1.6)	109.8, CH	6.96, br s
3″	146.7, C		146.9, C	
4″	145.6, C		145.8, C	
5″	114.1, CH	6.89, d (8.1)	114.3, CH	6.89, overlap
6″	121.0, CH	6.92, dd (8.1, 1.6)	120.8, CH	6.89, overlap
7″	82.9, CH	4.48, d (4.9)	83.6, CH	4.51, d (6.0)
8″	82.4, CH	4.65, overlap	82.2, CH	4.65, td (6.0, 3.9)
9″	64.5, CH_2	4.65, overlap	64.5, CH_2	Ha: 4.43, dd (11.8, 3.9) Hb: 4.32, dd (11.8, 6.0)
1‴	130.3, C		129.9, C	
2‴, 6‴	129.7, CH	8.08, br d (8.3)	129.7, CH	8.08, br d (7.7)
3‴, 5‴	128.5, CH	7.45, br t (8.3)	128.5, CH	7.45, br t (7.7)
4‴	133.1, CH	7.56, br t (8.3)	133.1, CH	7.57, br t (7.7)
7‴	166.6, C		166.6, C	
3-OCH_3	55.8, CH_3	3.70, s	55.8, CH_3	3.74, s
3″-OCH_3	56.0, CH_3	3.85, s	56.0, CH_3	3.82, s
7″-OCH_3	57.3, CH_3	3.31, s	57.3, CH_3	3.32, s

one carbonyl and seven olefinic). The NMR spectra demonstrate similarities to those of **8**, containing two phenylpropanoid units and a benzoic ester. However, the connectivity of two phenylpropanoids differs. This structural arrangement was confirmed through ^{1}H–^{1}H COSY correlations (Fig. 3) of H-9″/H-8″/H-7″, and H-9/H-8/H-7, and HMBC correlations (Fig. 3) of H-7/C-9, C-1, C-2, C-6, H-7″/C-1″, C-2″, C-6″, and H-2′, H-6′, H-9/C-7′. Furthermore, HMBC of H_2-9″/C-4, and H-9/C-7′ indicated that these three aromatic units are connected by C-4–O–C-9″ and C-9–O–C-7′ bonds. The planar structure of **9** was thus determined, with the relative configuration of H-7″ and H-8″ assigned based on their coupling constants. The larger coupling constant of H-7″/H-8″ ($J_{7'',8''}$ = 7.6 Hz) suggested their exposition as a *threo* form. The absolute configuration could not be determined due to insufficient quantity of compound **9**. The structure was ultimately con-

Table 5 ^{1}H (600 MHz) and ^{13}C NMR (150 MHz) data for **8** and **9** (*J* in Hz, in $CDCl_3$).

No.	8		9	
	δ_C	δ_H	δ_C	δ_H
1	132.3, C		130.3, C	
2	110.4, CH	7.04, d (1.9)	109.5, CH	6.95, d (2.0)
3	150.5, C		149.9, C	
4	146.2, C		148.5, C	
5	119.0, CH	6.86, d (8.3)	114.1, CH	6.70, d (8.2)
6	119.9, CH	6.92, dd (8.3, 1.9)	120.1, CH	6.87, dd (8.2, 2.0)
7	134.0, CH	6.70, d (15.9)	134.3, CH	6.65, br d (15.8)
8	122.7, CH	6.33, dt (15.9, 6.4)	121.6, CH	6.28, dt (15.8, 6.6)
9	65.6, CH_2	4.98, d (6.4)	65.8, CH_2	4.96, br d (6.6)
1′	130.3, C		130.2, C	
2′, 6′	129.8, CH	8.08, br d (7.7)	129.8, CH	8.08, br d (8.5)
3′, 5′	128.5, CH	7.45, br t (7.7)	128.5, CH	7.45, br t (8.5)
4′	133.1, CH	7.57, br t (7.4)	133.1, CH	7.56, br t (8.5)
7′	166.6, C		166.6, C	
1″	143.7, C		129.8, C	
2″	136.5, C		120.7, CH	6.83, d (2.0)
3″	148.2, C		146.7, C	
4″	105.4, CH	6.68, d (1.9)	145.4, C	
5″	132.6, C		109.5, CH	6.87, d (8.0)
6″	111.0, CH	6.54, d (1.9)	120.7, CH	6.84, dd (8.0, 2.0)
7″	84.4, CH	4.46, d (6.6)	84.1, CH	4.31, d (7.6)
8″	138.6, CH	5.85, ddd (17.0, 10.3, 6.6)	74.4, CH	4.02, ddd (7.6, 5.4, 3.0)
9″	116.5, CH_2	5.19, m	70.0, CH_2	Ha: 3.97, dd (10.2, 3.0) Hb: 3.73, dd (10.2, 5.4)
3-OCH_3	56.1, CH_3	3.89, s	56.0, CH_3	3.87, s
3″-OCH_3	56.4, CH_3	3.92, s	55.9, CH_3	3.79, s
7″-OCH_3	56.4, CH_3	3.27, s	56.9, CH_3	3.28, s
2″-OH		5.85, s		

firmed and designated as succignan D.

2.2. Biological activity

Chronic kidney disease (CKD) is characterized by excessive accumulation of extracellular matrix (ECM) [20]. Numerous studies have identified transforming growth factor-β1 (TGF-β1) as the principal pathogenic factor in glomerular and tubulointerstitial fibrosis [21]. In this study, TGF-β1-activated normal rat kidney proximal tubular epithelial cells (NRK-52e) were utilized to induce fibrosis, followed by assessment of ECM proteins including fibronectin, collagen I, and α-smooth muscle actin (α-SMA) to evaluate fibrosis progression. A Cell Count Kit-8 (CCK-8) assay was performed to exclude the possibility that the compounds' biological effects resulted from cytotoxicity. Results revealed that, except for compound **1** at 20 μmol·L^{-1}, none of the compounds exhibited significant cytotoxic effects (Fig. 6A). Compound **1** demonstrated no toxicity at 10 μmol·L^{-1} (Fig. 6B). Subsequently, non-toxic concentrations of the compounds were evaluated for their anti-fibrotic properties. Initial assessment revealed that compounds **6** and **7** at 20 μmol·L^{-1} effectively suppressed the expressions of α-SMA, collagen I, and fibronectin in TGF-β1-stimulated NRK-52e cells (Fig. 7). Further dose-response analysis demonstrated enhanced anti-fibrotic activity with increasing concentrations of (−)-**6** and (+)-**6** (Figs. 8A–8D). Additionally, TGF-β1-induced expression of α-SMA, collagen I and fibronectin in NRK-52e cells decreased progressively with increasing concentrations of (−)-**7** and (+)-**7**. (Figs. 8E–8H).

3. Experimental

3.1. General

The ultraviolet (UV) spectra were recorded using a Shimadzu UV-2401PC spectrometer (Agilent Technologies, Santa Clara, CA, USA). An Anton Paar MCP-100 digital polarimeter (Anton Paar, Austria) was employed for measuring optical rotations. Circular dichroism (CD) measurements were conducted using a JASCO J-815 CD spectrometer (JASCO, Japan). NMR spectra were obtained on a Bruker Avance 600 MHz spectrometer (Bruker, Karlsruhe, Germany) with TMS as the internal standard. HR-ESI-MS data were collected using a Shimadzu LC-20AD AB SCIEX triple TOF X500R MS spectrometer (Shimadzu Corporation, Tokyo, Japan). Column chromatography (CC) utilized C-18 silica gel (40–60 μm; Daiso Co., Japan), MCI gel CHP 20P (75–150 μm, Mitsubishi Chemical Industries, Tokyo, Japan), and Sephadex LH-20 (Amersham Pharmacia, Uppsala, Sweden). Semi-preparative high-performance liquid chromatography (HPLC) was performed using a Saipuruisi (SEP) chromatograph equipped with a YMC-Pack ODS-A column (250 mm × 10 mm, i.d., 5 μm). Preparative HPLC employed a SEP chromatograph with a YMC-Actus ODS-A column (250 mm × 20 mm, i.d., 5 μm). Racemic compounds were purified using chiral HPLC with Daicel Chiralpak columns (IC, 250 mm × 4.6 mm, i.d., 5 μm; 250 mm × 10 mm, i.d., 5 μm, and AD-H, 250 mm × 4.6 mm, i.d., 5 μm).

3.2. Material

Succinum was acquired from Guangdong Podik Cultural Creativity Co., Ltd. (Dongguan, China). The morphological characteristics of succinum are illustrated in Fig. 1. The voucher specimen (CHYX0673) has been deposited at the School of Pharmacy, Shenzhen University Medical School, China.

3.3. Extraction and isolation

Succinum (29.0 kg) was extracted with CH_2Cl_2 (2 × 150 L, 24 h), yielding 5.1 kg of crude extract. The extract was fractionated on an MCI gel CHP 20P column using gradient aqueous MeOH/^{i}PrOH (10∶1) (85%–100%), resulting in nine portions (Fr. 1–Fr. 9).

Nine fractions (Fr. 2.1–Fr. 2.9) were obtained by subjecting 450.0 g of Fr. 2 to an MCI gel CHP 20P column (MeOH/H_2O, 65%–100%). Fr. 2.6 (4.0 g) was chromatographed on Sephadex LH-20 (MeOH) to yield four parts (Fr. 2.6.1–Fr. 2.6.4). The seventh sub-fractions (Fr. 2.7, 7.0 g) were separated using semi-preparative HPLC (3.0 mL·min^{-1}) to obtain compounds **2** (6.2 mg, MeCN/H_2O, 30%, t_R 23.9 min), **3** (5.7 mg, MeCN/H_2O, 30%, t_R 22.2 min), and **4** (2.0 mg, MeCN/H_2O, 42%, t_R 10.3 min). Fr. 2.8 (13.8 g) underwent gel filtration on Sephadex LH-20 (MeOH), followed by semi-preparative HPLC purification (3.0 mL·min^{-1}), yielding compound **5** (1.0 mg, MeOH/H_2O, 56%, t_R 11.2 min).

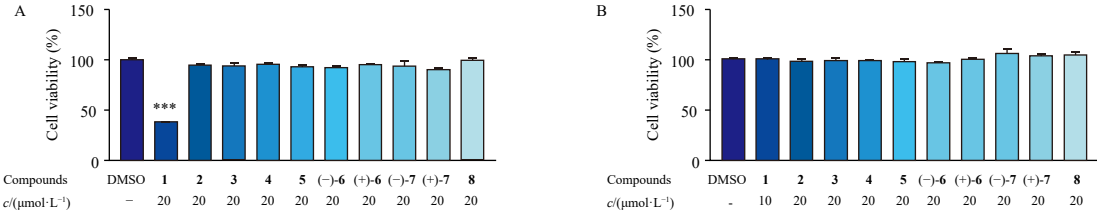

Fig. 6 NRK-52e cells proliferation in response to compounds by CCK-8 assay. (A) Cell viability of compounds **1**–**8** at 20 μmol·L^{-1} was examined. (B) Cell viability of compound **1** at 10 μmol·L^{-1} and compounds **2**–**8** at 20 μmol·L^{-1} was examined. Data are represented as mean ± SEM (n = 6). $^{***}P$ < 0.001 *vs* DMSO alone.

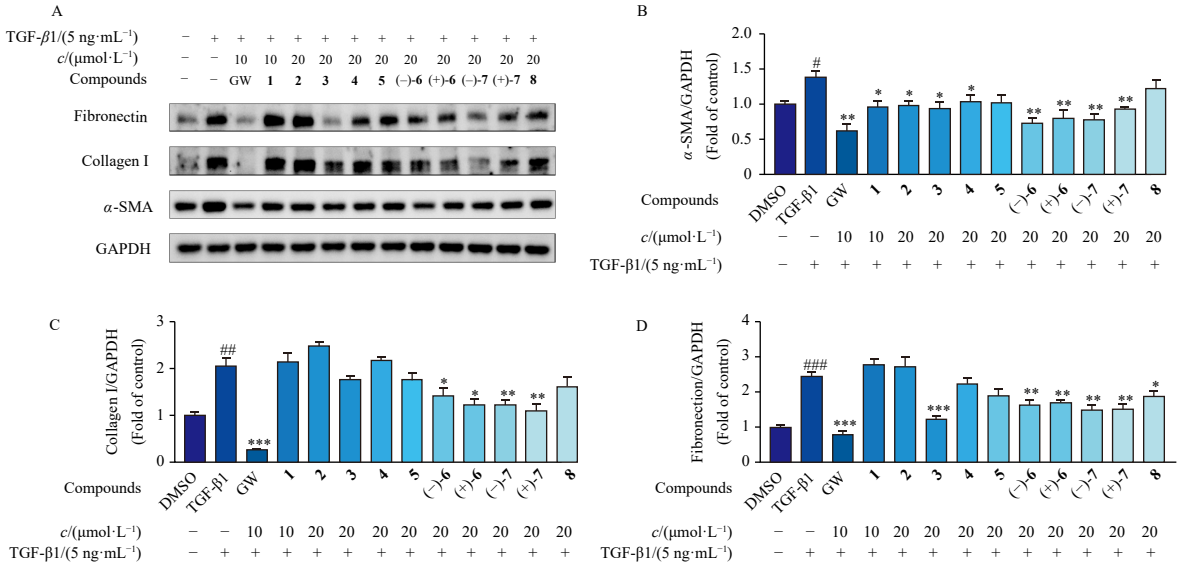

Fig. 7 Compounds inhibit renal fibrosis in TGF-β1-induced NRK-52e cells. Cells were incubated with compounds **1**–**8** for 1 h and then exposed to 5 ng·mL^{-1} TGF-β1 for 48 h. (A–D) The protein levels of α-SMA, collagen I, and fibronectin were determined by Western blotting, with GAPDH used as a control. Data are represented as mean ± SEM (n = 3). $^{\#}P$ < 0.05, $^{\#\#}P$ < 0.01, $^{\#\#\#}P$ < 0.001 *vs* DMSO alone; $^{*}P$ < 0.05, $^{**}P$ < 0.01, $^{***}P$ < 0.001 *vs* TGF-β1 alone. GW788388 (GW) was used as a positive control.

Fr. 6 (299.8 g) was separated into seven fractions (Fr. 6.1–Fr. 6.7) using an MCI gel CHP 20P column MeOH/^{i}PrOH (15∶1) (88%–100%). Fr. 6.5 (4.7 g) underwent purification through silica gel CC followed by semi-preparative HPLC (3.0 mL·min^{-1}), yielding compounds **1** (3.2 mg, MeCN/H_2O, 93%, t_R 31.3 min) and **9** (1.3 mg, MeCN/H_2O, 58%, t_R 21.6 min). Fr. 6.6 (67.4 g) underwent chromatographic separation on a silica gel column using CH_2Cl_2/MeOH gradient system (100∶1–5∶1), yielding fourteen fractions (Fr. 6.6.1–Fr. 6.6.14). Fr. 6.6.5 (8.0 g) underwent further purification by RP-18 CC using MeOH/H_2O (86%–100%) to produce seven parts (Fr. 6.6.5.1–Fr. 6.6.5.7). Following additional purification *via* semi-preparative HPLC (MeCN/H_2O 80%, 3.0 mL·min^{-1}), Fr. 6.6.5.7 (541.0 mg) yielded **6** (15.5 mg, t_R 18.2 min), **7** (27.1 mg, t_R 16.5 min) and **8** (2.1 mg, t_R 12.3 min).

Subsequently, racemic **6** and **7** underwent chiral HPLC separation to obtain their respective enantiomers, (−)-**6** (4.8 mg, t_R 23.0 min) and (+)-**6** (4.6 mg, t_R 25.3 min) (MeCN/H_2O, 60%, 1.0 mL·min^{-1}); (−)-**7** (3.9 mg, t_R 21.9 min) and (+)-**7** (3.7 mg, t_R 23.9 min) (MeCN/H_2O, 60%, 1.0 mL·min^{-1}).

3.4. Compound characterization

Succipenoid D (**1**): colorless oil; $[\alpha]_D^{25}$ +13.3 (c 0.15, MeOH); CD (MeOH) $\Delta\varepsilon_{204}$ −1.42, $\Delta\varepsilon_{214}$ −3.26, $\Delta\varepsilon_{238}$ −0.27; UV (MeOH) λ_{max} (log ε) 221 (1.98) nm; (+)HR-ESI-MS m/z 313.2523 [M + H]$^+$ (Calcd. for $C_{22}H_{33}O$, 313.2526); ^{1}H and ^{13}C NMR data (Table 1).

Succipenoid E (**2**): colorless oil; $[\alpha]_D^{25}$ −42.9 (c 0.14, MeOH); CD (MeOH) $\Delta\varepsilon_{204}$ −0.41, $\Delta\varepsilon_{220}$ +0.94, $\Delta\varepsilon_{244}$ −1.20, $\Delta\varepsilon_{261}$ −0.26; UV (MeOH) λ_{max} (log ε) 235 (2.45) nm; (+)HR-ESI-MS m/z 249.1843 [M + H]$^+$ (Calcd. for $C_{16}H_{25}O_2$, 249.1849); ^{1}H and ^{13}C NMR data (Table 2).

Succipenoid F (**3**): colorless oil; $[\alpha]_D^{25}$ −46.7 (c 0.15, MeOH); CD (MeOH) $\Delta\varepsilon_{208}$ +0.27, $\Delta\varepsilon_{215}$ +1.77, $\Delta\varepsilon_{233}$ −3.61, $\Delta\varepsilon_{265}$ +0.15; UV (MeOH) λ_{max} (log ε) 232 (2.97) nm; (+)HR-ESI-MS m/z 249.1844 [M + H]$^+$ (Calcd. for $C_{16}H_{25}O_2$, 249.1849); ^{1}H and ^{13}C NMR data (Table 2).

Succipenoid G (**4**): colorless oil; $[\alpha]_D^{25}$ +33.3 (c 0.15, MeOH); CD (MeOH) $\Delta\varepsilon_{205}$ +1.11, $\Delta\varepsilon_{220}$ +4.08, $\Delta\varepsilon_{251}$ −0.76; UV (MeOH) λ_{max} (log ε) 221 (2.09) nm; (+)HR-ESI-MS m/z 265.1789 [M + H]$^+$ (Calcd. for $C_{16}H_{25}O_3$, 265.1798); ^{1}H and ^{13}C NMR data, see Table 3.

Succipenoid H (**5**): colorless oil; $[\alpha]_D^{25}$ +3.7 (c 0.27, MeOH); CD (MeOH) $\Delta\varepsilon_{213}$ −0.92, $\Delta\varepsilon_{217}$ +0.10, $\Delta\varepsilon_{223}$ −0.87, $\Delta\varepsilon_{242}$ +0.11; UV (MeOH) λ_{max} (log ε) 230 (1.67) nm; (+)HR-ESI-MS m/z 239.1642 [M + H]$^+$ (Calcd. for $C_{14}H_{23}O_3$, 239.1642); ^{1}H and ^{13}C NMR data, see Table 3.

(±)-Succignan A (**6**): yellowish oil; {$[\alpha]_D^{25}$ +23.0 (c 0.11, MeOH); CD (MeOH) $\Delta\varepsilon_{200}$ +33.41, $\Delta\varepsilon_{209}$ −6.52, $\Delta\varepsilon_{219}$ +2.08, $\Delta\varepsilon_{231}$ −2.72; (+)-**6**}; {$[\alpha]_D^{25}$ −17.5 (c 0.11, MeOH); CD (MeOH) $\Delta\varepsilon_{200}$ −28.81, $\Delta\varepsilon_{211}$ +3.17, $\Delta\varepsilon_{221}$ −0.93, $\Delta\varepsilon_{234}$ +0.68; (−)-**6**}; UV (MeOH) λ_{max} (log ε) 230 (3.09), 272 (2.64) nm; (+)HR-ESI-MS m/z 621.2076 [M + Na]$^+$ (Calcd. for $C_{35}H_{34}O_9Na$, 621.2095); ^{1}H and ^{13}C NMR data (Table 4).

(±)-Succignan B (**7**): yellowish oils; {$[\alpha]_D^{25}$ +9.6 (c 0.15, MeOH); CD (MeOH) $\Delta\varepsilon_{202}$ −38.04, $\Delta\varepsilon_{207}$ +2.53, $\Delta\varepsilon_{220}$ −1.43, $\Delta\varepsilon_{237}$ +1.11; (+)-**7**}; {$[\alpha]_D^{25}$ −11.7 (c 0.17, MeOH); CD (MeOH) $\Delta\varepsilon_{200}$ +36.21, $\Delta\varepsilon_{210}$ −2.78, $\Delta\varepsilon_{220}$ +0.92, $\Delta\varepsilon_{233}$ −2.49; (−)-**7**}; UV (MeOH) λ_{max} (log ε) 228 (3.42), 268 (2.96) nm; (+)HR-ESI-MS m/z 621.2074 [M + Na]$^+$ (Calcd. for $C_{35}H_{34}O_9Na$, 621.2095); ^{1}H and ^{13}C NMR data (Table 4).

Succignan C (**8**): yellowish oil; $[\alpha]_D^{25}$ −8.3 (c 0.13, MeOH); CD

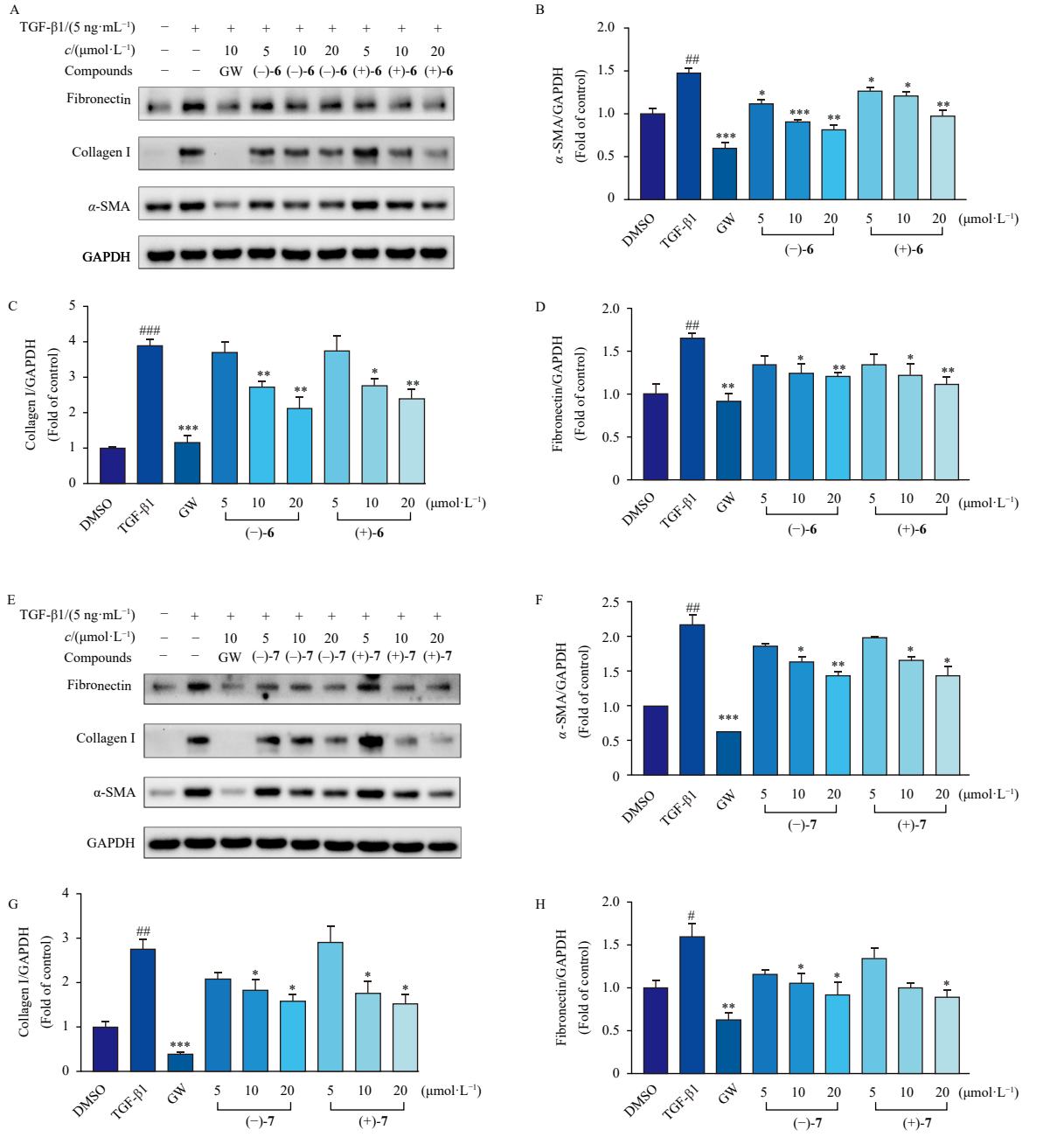

Fig. 8 Compounds **6** and **7** inhibit renal fibrosis in TGF-β1-induced NRK-52e cells. Cells were incubated in different concentrations of compounds **6** (A–D) and **7** (E–H) for 1 h and then exposed to 5 ng·mL^{-1} TGF-β1 for 48 h. The protein levels of *α*-SMA, collagen I, and fibronectin were determined by Western blotting, with GAPDH used as a control. Data represent mean ± SEM (n = 3). $^{\#}P < 0.05$, $^{\#\#}P < 0.01$, $^{\#\#\#}P < 0.001$ *vs* DMSO alone; $^{*}P < 0.05$, $^{**}P < 0.01$, $^{***}P < 0.001$ *vs* TGF-β1 alone. GW was used as a positive control.

(MeOH) $\Delta\varepsilon_{205}$ +20.84, $\Delta\varepsilon_{210}$ −4.40, $\Delta\varepsilon_{214}$ +8.58, $\Delta\varepsilon_{221}$ −2.52; UV (MeOH) λ_{max} (log ε) 264 (3.00) nm; (+)HR-ESI-MS *m/z* 499.1733 $[M + Na]^+$ (Calcd. for $C_{28}H_{28}O_7Na$, 499.1727); ^1H and ^{13}C NMR data (Table 5).

Succignan D (**9**): yellowish oil; UV (MeOH) λ_{max} (log ε) 226 (3.20), 269 (2.82) nm; (+)HR-ESI-MS *m/z* 517.1819 $[M + Na]^+$ (Calcd. for $C_{28}H_{30}O_8Na$, 517.1833); ^1H and ^{13}C NMR data (Table 5).

3.5. Biological assays of compounds

3.5.1. Cell culture

NRK-52e cells (Cell Bank of China Science Academy, Shanghai, China) were maintained in high glucose Dulbecco's modified Eagle medium (DMEM) (C11995500BT, Gibco, USA) supplemented with 10% fetal bovine serum (FBS) (2094468CP, Gibco, USA), 100 U·mL^{-1} penicillin and 100 μg·mL^{-1} streptomycin in a humidified atmosphere containing 5% CO_2 at 37 °C.

3.5.2. Cell viability assay

NRK-52e cells (5 × 10^4 cells/mL) were seeded in 96-well plates with complete DMEM and incubated for 24 h. Subsequently, the cells were treated with various concentrations of compounds or DMSO for 48 h. Following treatment, CCK-8 (Beyotime, Shanghai, China) was added to each well and incubated at 37 °C for 1 h. The absorbance was measured at 450 nm using a microplate reader (BioTek, USA).

3.5.3. Western blotting analysis

NRK-52e cells were plated at a concentration of 5 × 10^4 cells/mL in 2 mL per well in 6-well dishes and incubated overnight. Following a 6 h starvation period, the cells were exposed to various concentrations of compounds **1**–**8** or DMSO in

DMEM with 4% FBS for 48 h. Subsequently, recombinant TGF-β1 at 5 ng·mL^{-1} was introduced to each well to stimulate cell fibrosis. Total protein was extracted from the cell lines using radio immunoprecipitation assay (RIPA) buffer (Beyotime, Shanghai, China) containing protease and phosphatase inhibitor cocktail (Roche, Germany). The protein samples were then quantified using a BCA assay (Thermo Fisher Scientific, USA). Western blotting analysis was performed following the established protocol of our research group [22].

The primary antibodies utilized in this study included anti-fibronectin (dilution 1∶1000; ab268020; Abcam), anti-collagen I (1∶1000 dilution; ab270993; Abcam), anti-α-SMA (1∶1000 dilution; A2547; Sigma), and anti-glyceraldehyde-3-phosphate dehydrogenase (GAPDH) (1∶2000 dilution; sc-365062; Santa Cruz).

3.5.4. Statistical analysis

Data analysis was performed using IBM SPSS Statistics 22, and results were expressed as mean ± standard error of mean (SEM). Comparisons between groups were conducted using one-way ANOVA, followed by Student-Newman-Kuels test. $P < 0.05$ was considered statistically significant. Specific statistical tests were detailed in figure legends for each experiment.

4. Conclusion

In conclusion, this study isolated five previously undescribed diterpenoids and four undescribed lignans from succinum. Spectroscopic and computational methods were employed to determine their structures, including absolute configurations, thereby enhancing understanding of succinum's chemical composition. Furthermore, biological evaluation of the isolates revealed that compounds **6** and **7** inhibit the expression of α-SMA, collagen I, and fibronectin in NRK-52e cells stimulated by TGF-β1, suggesting their potential for treating renal fibrosis. This study provides new insights into succinum's chemical and biological profiles.

Funding

The work was supported by Shenzhen Fundamental Research Program (No. JCYJ20200109114003921).

Declaration of competing interest

The authors declare no competing financial interests.

References

1 Lambert JB, Poinar GO. Amber: the organic gemstone. *Acc Chem Res*. 2002;35:628-636. https://doi.org/10.1021/ar0001970.
2 Zhong HB. Amber resources in China. *J Gems Gemmol*, 2003;5(2):33. https://doi.org/10.15964/j.cnki.027jgg.2003.02.012.
3 Panczak J, Kosakowski P, Zakrzewski A. Biomarkers in fossil resins and their palaeoecological significance. *Earth-Sci Rev*. 2023;242:104455. https://doi.org/10.1016/j.earscirev.2023.104455.
4 Yamamoto S, Otto A, Krumbiegel G, et al. The natural product biomarkers in succinite, glessite and stantienite ambers from Bitterfeld, Germany. *Rev Palaeobot Palyno*. 2006;140:27-49. https://doi.org/10.1016/j.revpalbo.2006.02.002.
5 Cheng S, Luo X, Wang W, et al. Comparison and identification of succinum and its adulterants. *Chin J Pharm*. 2014;45(10):933-935. https://doi.org/10.16522/j.cnki.cjph.2014.10.021.
6 Wei C, Zhu Z, Zheng JN, et al. Chinese medicine, succinum, ameliorates cognitive impairment of carotid artery ligation rats and inhibits apoptosis of HT22 hippocampal cells *via* regulation of the GSK3β/*β*-catenin pathway. *Front Pharmacol*. 2022;13:867477. https://doi.org/10.3389/fphar.2022.867477.
7 Shevchenko M, Sukhikh S, Babich O, et al. First insight into the diversity and antibacterial potential of psychrophilic and psychotrophic microbial communities of abandoned amber quarry. *Microorganisms*. 2021;9:1521. https://doi.org/10.3390/microorganisms9071521.
8 Tian Y, Zhou SQ, Takeda R, et al. Anti-inflammatory activities of amber extract in lipopolysaccharide-induced RAW 264.7 macrophages. *Biomed Pharmacother*. 2021;141:111854. https://doi.org/10.1016/j.biopha.2021.111854.
9 Maruyama M, Kobayashi M, Uchida T, et al. Anti-allergy activities of Kuji amber extract and kujigamberol. *Fitoterapia*. 2018;127:263-270. https://doi.org/10.1016/j.fitote.2018.02.033.
10 Liu YY, Yan YM, Wang DW, et al. Populusene A, an anti-inflammatory diterpenoid with a bicyclo[8,4,1]pentadecane scaffold from *Populus euphratica* resins. *Org Lett*. 2021;23:8657-8661. https://doi.org/10.1021/acs.orglett.1c02378.
11 Sura MB, Zhu YX, Cheng YX. X-ray study of cembranoids with flexible rings from *Boswellia papyrifera* resins allowing structural revision of misleading structures from the past 70 years. *Chem Eur J*. 2023;29:e202300559. https://doi.org/10.1002/chem.202300559.
12 Wang YF, Fang HB, Yan YM, et al. Succipenoids A–C: a dimeric abietane and nor-abietane diterpenoids from fossil Chinese medicinal succinum and their anti-inflammatory potential. *Phytochemistry*. 2023;215:113835. https://doi.org/10.1016/j.phytochem.2023.113835.
13 Butler MS, Capon RJ. The luffarins (A–Z), novel terpenes from an Australian marine sponge, *Luffariella geometrica*. *Aust J Chem*. 1992;45:1705-1743. https://doi.org/10.1071/CH9921705.
14 Helmlinger D, Frater G. Rearrangement of sclareolide to (4.3.3)-propellanes under strongly acidic conditions. *Tetrahedron Lett*. 1992;33:6119-6122. https://doi.org/10.1016/S0040-4039(00)60021-7.
15 Wang F, Zhang L, Zhang Q, et al. Neolignan and phenylpropanoid compounds from the resin of *Styrax tonkinensis*. *J Asian Nat Prod Res*. 2021;23:527-535. https://doi.org/10.1080/10286020.2021.1910240.
16 Xu K, Yang PF, Yang YN, et al. Direct assignment of the *threo* and *erythro* configurations in polyacetylene glycosides by ^{1}H NMR spectroscopy. *Org Lett*. 2017;19:686-689. https://doi.org/10.1021/acs.orglett.6b03855.
17 Xiong L, Zhu CG, Li YR, et al. Lignans and neolignans from *Sinocalamus affinis* and their absolute configurations. *J Nat Prod*. 2011;74:1188-1200. https://doi.org/10.1021/np200117y.
18 Li Q, Li JJ, Bao XH, et al. Unusual sesquilignans with anti-inflammatory activities from the resin of *Ferula sinkiangensis*. *Bioorg Chem*. 2022;127:105986. https://doi.org/10.1016/j.bioorg.2022.105986.
19 Costa-Silva TA, Grecco SS, de Sousa FS, et al. Immunomodulatory and antileishmanial activity of phenylpropanoid dimers isolated from *Nectandra leucantha*. *J Nat Prod*. 2015;78:653-657. https://doi.org/10.1021/np500809a.
20 Rayego-Mateos S, Campillo S, Rodrigues-Diez RR, et al. Interplay between extracellular matrix components and cellular and molecular mechanisms in kidney fibrosis. *Clin Sci*. 2021;135:1999-2029. https://doi.org/10.1042/CS20201016.
21 Gifford CC, Tang J, Costello A, et al. Negative regulators of TGF-β1 signaling in renal fibrosis; pathological mechanisms and novel therapeutic opportunities. *Clin Sci*. 2021;135:275-303. https://doi.org/10.1042/CS20201213.
22 Huang XL, Zhou YT, Yan YM, et al. Sesquiterpenoid-chromone heterohybrids from agarwood of *Aquilaria sinensis* as potent specific smad3 phosphorylation inhibitors. *J Org Chem*. 2022;87:7643-7648. https://doi.org/10.1021/acs.joc.2c00145.